ELSEVIER

Journal of Neuroscience Methods 111 (2001) 59–66

JOURNAL OF NEUROSCIENCE METHODS

www.elsevier.com/locate/jneumeth

A sequential protocol combining dual neuroanatomical tract-tracing with the visualization of local circuit neurons within the striatum

Nancy Gonzalo [a], Ainhoa Moreno [a], María A. Erdozain [a], Pedro García [a], Alfonso Vázquez [a,b], María Castle [a], José L. Lanciego [a,*]

[a] *Departamento de Anatomía, Facultad de Medicina, Universidad de Navarra, Pamplona, Spain*
[b] *Servicio de Neurocirugía, Hospital de Navarra, Irunlarrea s/n, 31080 Pamplona, Spain*

Received 21 May 2001; received in revised form 11 July 2001; accepted 13 July 2001

Abstract

We describe here an experimental approach designed to aid in the identification of complex brain circuits within the rat corpus striatum. Our aim was to characterize in a single section (i) striatal thalamic afferents, (ii) striatopallidal projection neurons and (iii) striatal local circuit interneurons. To this end, we have combined anterograde tracing using biotinylated dextran amine and retrograde neuroanatomical tracing with Fluoro-Gold. This dual tracing protocol was further implemented with the visualization of different subpopulations of striatal interneurons. The subsequent use of three different peroxidase substrates enabled us to unequivocally detect structures that were labeled within a three-color paradigm.

Keywords: Dextran amine; Fluoro-Gold; Diaphorase; Interneuron; Peroxidase; Basal ganglia

1. Introduction

The striatum is the structure that receives the majority of the inputs of the basal ganglia, principally from the entire cerebral cortex, the thalamus, dopaminergic projections from the substantia nigra compacta and serotoninergic fibers from the dorsal raphe nuclei. Once processed within the striatum, the information is conveyed to the entopeduncular nucleus and the substantia nigra reticulata (the so-called 'direct pathway') or to the lateral globus pallidum, giving rise to the 'indirect pathway' (for a review, see Albin et al., 1989; Smith et al., 1998). The striatum consists of both projection neurons and interneurons. Projection neurons are medium-sized spiny cells, comprising up to 95% of the total striatal neuronal population in rodents (Wilson and Groves, 1980; Chang et al., 1982). Several types of striatal interneuron have been described to date (Kawaguchi et al., 1995), including large cholinergic interneurons (ChAT-ir; Lehmann and Langer, 1983; Satoh et al., 1983; Vincent et al., 1983a,b; Bolam et al., 1984), GABAergic interneurons immunoreactive for the calcium binding proteins parvalbumin (PV-ir; Cowan et al., 1990; Kita et al., 1990) or calretinin (CR-ir; Bennett and Bolam, 1993; Figueredo-Cárdenas et al., 1996a; Mura et al., 2000), and interneurons expressing the enzyme nitric oxide synthase (NOS) as well as nicotinamide adenine dinucleotide phosphate-diaphorase (NADPH-d), somatostatin, neuropeptide Y and calbindin (Bolam et al., 1983; Scherer-Singler et al., 1983; Vincent and Johansson, 1983; Vincent et al., 1983a,b; Sandell et al., 1986; Kowall et al., 1987; Kita and Kitai, 1988; Hope and Vincent, 1989; Kawaguchi et al., 1995; Rushlow et al., 1995; Figueredo-Cárdenas et al., 1996b; Wu and Parent, 2000).

The way in which the received information is processed within the striatum remains poorly understood. Extensive research has been carried out in recent years to reveal the arrangement of striatal microcircuits in which local circuit neurons were seen to play a key role.

* Corresponding author. Tel.: +34-948-425600x6235; fax: +34-948-425649.
E-mail address: jlanciego@unav.es (J.L. Lanciego).

0165-0270/01/$ - see front matter
PII: S0165-0270(01)00440-X

Projections coming from the cerebral cortex, the pars compacta of the substantia nigra and the thalamus are known to synapse both on projection neurons and interneurons (Kubota et al., 1987; Vuillet et al., 1990; Lapper and Bolam, 1992; Lapper et al., 1992; Dimova et al., 1993; Bennett and Bolam, 1994; Kachidian et al., 1996, 1998; Sidibé and Smith, 1996, 1999; Koós and Tepper, 1999; Rudkin and Sadikot, 1999). Striatal inputs may influence the striatal output through directing their contacts onto striatal projection neurons or by exciting the interneurons which synchronize the discharge of several striatal projection neurons (Koós and Tepper, 1999). It has been suggested that interneurons relay incoming information to spiny cells, in the form of inhibition or modulation. Indeed, the inhibitory discharges from a single interneuron are powerful enough to block the generation of action potentials in a large number of spiny striatofugal neurons.

The technique that we describe here offers a powerful approach for the analysis of detailed extrinsic circuitry. The inherent complexity of striatal microcircuits requires the design of protocols that facilitate the combination of existing methods. The primary objective of the methodology presented here was to reliably and simultaneously stain afferent fibers, efferent neurons and interneurons. Thalamostriatal projections arising from the parafascicular nucleus were chosen as the striatal afferents to be studied (Sadikot et al., 1990, 1992a,b; Deschênes et al., 1996), and were labeled by means of the anterogradely transported tracer biotinylated dextran amine. A subpopulation of striatal neurons involved in the direct pathway was retrogradely labeled after the delivery of Fluoro-Gold in the entopeduncular nucleus. Finally, the four main types of striatal interneurons were identified immunocytochemically using specific antisera against ChAT, PV or CR, or histochemically (visualized with the 'diaphorase' staining).

2. Material and methods

Female Wistar rats with a body weight ranging from 240 to 280 g were used in this study. Animals were handled at all times according to the European Council Directive 86/609/EEC as well as to the Society for Neuroscience Policy on the Use of Animals in Neuroscience Research. Experiments were conducted under the approval of the Local Ethical Committee for Animal Testing of the University of Navarra (protocol No. 037/2000).

2.1. Surgery, survival time and perfusion

Animals were deeply anesthetized with an intramuscularly injected mixture of four parts of Ketaset (1% of a solution of ketamine, Aesco, Boxtel, The Netherlands) to three parts of Rompun (2% solution of xylazine, Bayer, Leverkusen, Germany). The rats were placed in a stereotaxic frame and the tracers were iontophoretically delivered in a single surgical session. Biotinylated dextran amine (BDA, Molecular Probes Europe, Leiden, The Netherlands) was injected in the parafascicular nucleus of the thalamus (Fig. 1B) as a 10% solution in 0.01 M phosphate buffer, pH 7.25 through a glass micropipette (inner tip diameter 25–40 μm). BDA delivery was achieved by using a 5 μA positive pulsed direct current (7 s on/off). Next, a 2% solution of Fluoro-Gold (FG, Fluorochrome, Englewood, CA, USA) in 0.1 M cacodylate buffer, pH 7.3, was delivered to the ipsilateral entopeduncular nucleus (Fig. 1A), using the same iontophoretic parameters described above for BDA injections. Stereotaxic coordinates were taken from the atlas of Paxinos and Watson (1998).

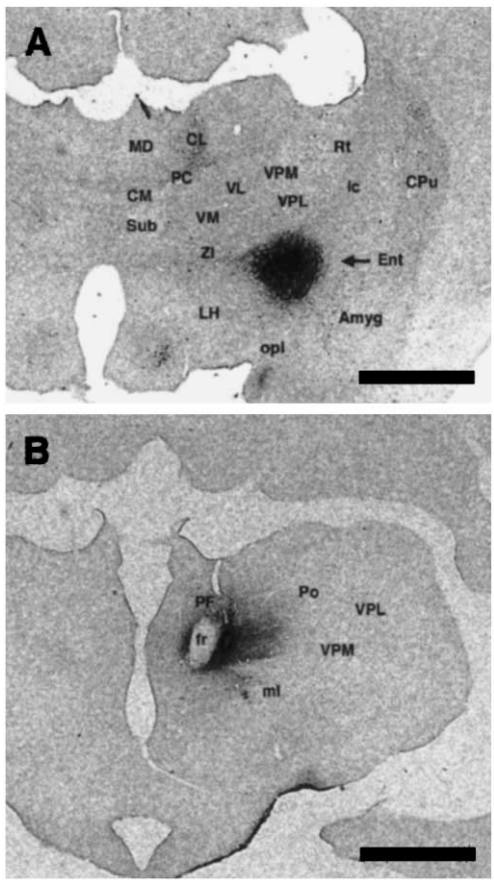

Fig. 1. Injection sites. (A) FG injection site located within the entopeduncular nucleus. Please note that the tracer deposit is confined within this nucleus, without spreading over neighboring nuclei. Scale bar = 1750 μm. (B) Low-power photomicrograph, taken from a coronal section through the posterior thalamus, illustrating a small BDA injection site located within the parafascicular nucleus. Scale bar = 1750 μm. Abbreviations taken from the atlas of Paxinos and Watson, 4th edition (1998).

After a survival time of 7 days, the animals were deeply anesthetized with an overdose of 10% chloral hydrate in distilled water and perfused transcardially. The perfusates consisted of a Ringer's saline rinsing solution (at body temperature), immediately followed by 500 ml of fixative containing 4% paraformaldehyde, 0.1% glutaraldehyde and 0.2% saturated picric acid in 0.125 M phosphate buffer, pH 7.4. After the perfusion, the skull was opened and the brain removed and stored in a cryoprotective solution (Rosene et al., 1986) containing 2% dimethylsulphoxide and 20% glycerin in 0.125 M phosphate buffer, pH 7.4. Coronal sections (40 μm-thick) were obtained and collected in 0.125 M phosphate buffer, pH 7.4.

2.2. Histology. I. Dual tracing with BDA and FG followed by the immunocytochemical detection of interneurons expressing either ChAT, PV or CR

Since a detailed protocol combining dual tracing with BDA and FG plus the detection of PV-ir neurons can be found elsewhere (Lanciego et al., 1997), the following protocol is focused on the histochemical detection of BDA, followed by two sequential PAP protocols for the detection of neurons expressing either ChAT or CR, and neurons containing FG.

Sections were first incubated in an ABC solution (ABC kit standard PK-4000; Vector Laboratories, Burlingame, CA) for 90 min at room temperature (Veenman et al., 1992), and then developed for 5–10 min with nickel-enhanced DAB (DAB-Ni; DAB from Sigma, St. Louis, MO), resulting in a black precipitate (Hancock, 1982). The DAB-Ni incubation solution was prepared by dissolving 0.2 g of nickel ammonium sulfate and 7.5 mg of DAB in 50 ml of 0.05 M Tris/HCl, pH 8. Immediately before use, 10 μl of 30% H_2O_2 was added. Subsequently, the sections were incubated in a solution containing 1:500 rabbit anti-ChAT (Chemicon, Temecula, CA) or 1:2000 rabbit anti-CR (Chemicon) for 60 h at 4 °C, then in a 1:50 swine anti-rabbit antiserum (Dako, Copenhagen, Denmark) for 2 h at room temperature, and finally in a peroxidase-anti-peroxidase complex (1:600 rabbit-PAP, Dako) for 90 min at room temperature. Localization of the antisera complexes was visualized with the chromogen DAB (20–40 min, room temperature), that forms a brown precipitate. The filtered DAB solution was prepared by dissolving 5 mg of DAB to 10 ml of 0.05 M Tris/HCl, pH 7.6, after which 3.3 μl of H_2O_2 was added. Finally, the sections were transferred to a solution containing 1:2000 rabbit anti-FG (Chemicon) for 60 h at 4 °C and then incubated in a bridge antiserum (swine anti rabbit; Dako) and in a PAP complex (rabbit-PAP; Dako), as described above for the immunocytochemical detection of ChAT or CR. Neurons displaying retrogradely transported FG were finally stained purple by using Vector® VIP peroxidase substrate (one drop of each vial to prepare 3.5 ml of working solution; then wait for 5–10 min).

2.3. Histology. II. NADPH-d histochemistry followed by dual tracing with BDA and FG

The histochemical detection of NADPH-diaphorase activity (Scherer-Singler et al., 1983; Hope and Vincent, 1989) was achieved by incubating the sections in a solution containing 8.3 mg of β-NADPH (Sigma), 9.84 mg of nitroblue-tetrazolium (NBT, Sigma) and 150 μl of 20% Triton X-100; all in 10 ml of 0.05 M Tris/HCl, pH 7.6, for 30 min at 36 °C, and monitored under intermittent microscopic examination. The NADPH-diaphorase system reduces the dye NBT to the insoluble blue reaction product. Next, the transported BDA was histochemically visualized with an ABC solution and stained brown using DAB. Finally, a PAP procedure was conducted for the detection of retrogradely transported FG, as described above (purple-stained neurons with V-VIP peroxidase substrate).

Once each particular staining sequence was completed, the sections were mounted on glass slides using a 2% solution of gelatin (Merck, Darmstadt, Germany) in 0.05 M Tris/HCl pH 7.6, dried at room temperature, rapidily dehydrated in toluene, and coverslipped with Entellan (Merck). All antisera used in this procedure were diluted in 0.05 M TBS, pH 8, with 0.5% Triton X-100 (TBS-Tx, Sigma). The incubations in the primary antisera were implemented with 2% of bovine serum albumin (BSA, Merck). Extensive washing with 0.05 M TBS-Tx, pH 8, was carried out throughout the procedure. Several rinsing steps with 0.05 M Tris/HCl, pH 7.6, were performed prior to and after the reactions in the different chromogen solutions.

Please note that toluene is a hazardous, highly toxic chemical and has to be handled with the appropriate care. The purple precipitate that belongs to V-VIP substrate is unstable under standard ethanol treatments. Therefore, toluene has to be used as an efficient alternative to ethanol for dehydration procedures. The final precipitate of the V-VIP substrate does not impose demands on the storage of the sections after staining. According to our experience, no fading of the V-VIP stain has been noticed after a 5 years storage of the sections under standard conditions (boxes, vertical storage containers, etc.) at room temperature.

3. Results

Two different staining procedures were tested in this study. The first approach was to visualize the transportation of BDA using an ABC solution and stained black using nickel-enhanced DAB (DAB-Ni), followed

by a PAP method to immunocytochemically detect either calretinin (CR), parvalbumin (PV) or choline-acetyl-transferase (ChAT), each marker being stained brown with DAB. Finally, another PAP method was carried out to immunocytochemically detect FG-containing neurons (stained purple with V-VIP). A different protocol was employed to detect neurons that contained the enzyme NADPH-d and it was coupled to the histochemical visualization of the anterogradely transported BDA and the immunocytochemical staining of retrogradely transported FG. The chromogens used being nitro blue tetrazolium (NTB, blue formazan reaction product), diaminobenzidine (DAB, brown precipitate) and Vector® VIP (V-VIP, purple color), respectively.

In all cases, FG labeled, striatopallidal-projecting neurons were unequivocally identified by using antisera against transported FG (Fig. 2A–2G), and purple stained with V-VIP substrate. These neurons displayed a typical granular appearance with the reaction product being mainly confined to the cytoplasm, although in some cases proximal dendrites were partially stained. Injections with BDA in the parafascicular thalamic nucleus (PF) resulted in the anterograde labeling of prominent projections that extended over broad territories of the rat striatum as described elsewhere (Herkenham and Pert, 1981; Deschênes et al., 1996). These projections were distributed in patches within the matrix compartment of the striatum (Fig. 2F), their location depending on the placement of the injection site within the PF nucleus. BDA labeling appeared as a homogeneous reaction product distributed throughout axons, axon collaterals and boutons, colored brown or black, depending on the method of visualization (Fig. 2A–D, F and G).

Four different subpopulations of interneurons within the striatum were identified in the present study, all of them displaying the classical morphological features and preferred distribution previously reported for these striatal interneurons (Kubota and Kawaguchi, 1993; Kawaguchi et al., 1995; Wu and Parent, 2000). In general, PV-ir neurons were the largest in diameter and CR-ir neurons were the smallest. The cell bodies and proximal dendrites were well stained in all cases, although some differences were noticed between the distinct labeled interneurons. Taken together, both PV-ir and CR-ir cells, as well as NADPH-d positive interneurons were readily identified in their respective series, contrasting well against the background stain and easily seen as distinct from FG labeled neurons and BDA labeled fibers. In contrast, problems were observed in staining the ChAT-ir interneurons (Fig. 2E). Although different antisera were tested under different conditions, we failed to identify the optimal conditions for reliable immunocytochemistry. In order to be able to clearly identify ChAT-ir neuronal profiles, DAB staining must be performed over a long time, sometimes hampering the visualization of FG-labeled neurons. Moreover, prolonged DAB incubations usually increases the risk 'color mixing phenomena' when using DAB chromogen and the DAB-Ni substrate (for more details, see Lanciego et al., 1997, 1998).

Irrespective of the methodology followed, all series succeed in demonstrating one source of afferent fibers to the striatum, one type of striatofugal projecting neuron and one subclass of striatal interneuron. The most successful combination is probably the one combining NADPH-d histochemistry, BDA histochemistry and FG immunocytochemistry (Fig. 2F & G). The discrimination of the colors between the blue (NBT), brown (DAB) and purple (V-VIP) precipitates is good enough to unequivocally identify each labeled element (NADPH-d interneurons, BDA fibers and FG neurons, respectively). Other options combining anterograde

Fig. 2. Striatal local circuit interneurons, efferent neurons and afferent fibers. (A) Low-power photomicrograph illustrating a dense plexus of BDA varicose fibers, stained black with nickel-enhanced DAB (DAB-Ni) and a calretinin positive interneuron (CR-ir) stained brown with DAB. Several striatofugal neurons were lightly labeled with Fluoro-Gold (FG) and stained purple with V-VIP. Scale bar = 50 μm. (B) Higher magnification photomicrograph taken from a different specimen illustrating the combination of BDA + CR + FG. CR-ir neurons are characterized by small somata and two to four long and thin sparsely branched dendrites. Scale bar = 25 μm. (C and D) Photomicrographs showing the outcome of the combination of BDA + PV + FG. Both BDA fibers (slightly out of focus) and FG neurons were stained as described in (A). This staining sequence was also carried out with the immunocytochemical detection of parvalbumin-containing interneurons (PV-ir; see brown arrows in 2C). PV-ir interneurons were the largest in diameter and were also characterized by the presence of thick principal dendrites, giving rise to numerous branches that could be followed over long distances. Scale bar is 35 μm in Fig. 2C and 25 μm in Fig. 2D. (E) The main drawbacks were found when trying to combine dual tracing with BDA and FG (black fibers and purple neuron -purple arrow-, respectively), with the immunocytochemical detection of ChAT-ir neurons. The unequivocal characterization of cholinergic interneurons often requires prolonged incubations in the DAB chromogen thereby leading to an increase in the amount of background stain. Scale bar = 25 μm. (F and G) Photomicrographs showing the outcome of a procedure designed for the histochemical detection of NADPH-d positive interneurons (by using the blue NTB substrate), combined with dual tracing with BDA and FG. Since the discrimination between the dark blue color that belongs to NADPH-d and the black-stained BDA fibers with DAB-Ni (as in our standard procedure) might be difficult at times (especially when dealing with thin NADPH-d positive dendrites and fibers), we used DAB without metallic enhancement to visualize BDA. BDA-labeled fibers were stained in brown, spreading over the matrix compartment of the striatum, without entering within the striosomes, as clearly seen in Fig. 2F. NADPH-d positive neurons were preferentially localized at the border between the striatal patch/matrix compartments, a typical feature shared with other subclasses of striatal interneurons (Kubota and Kawaguchi, 1993). The technical combination illustrated in Figs. 2F & G probably yielded the best results of all the protocols tested, affording a nice color discrimination between the chromogens involved and reduced background stain. Scale bar is 50 μm (Fig. 2F) and 25 μm (Fig. 2G).

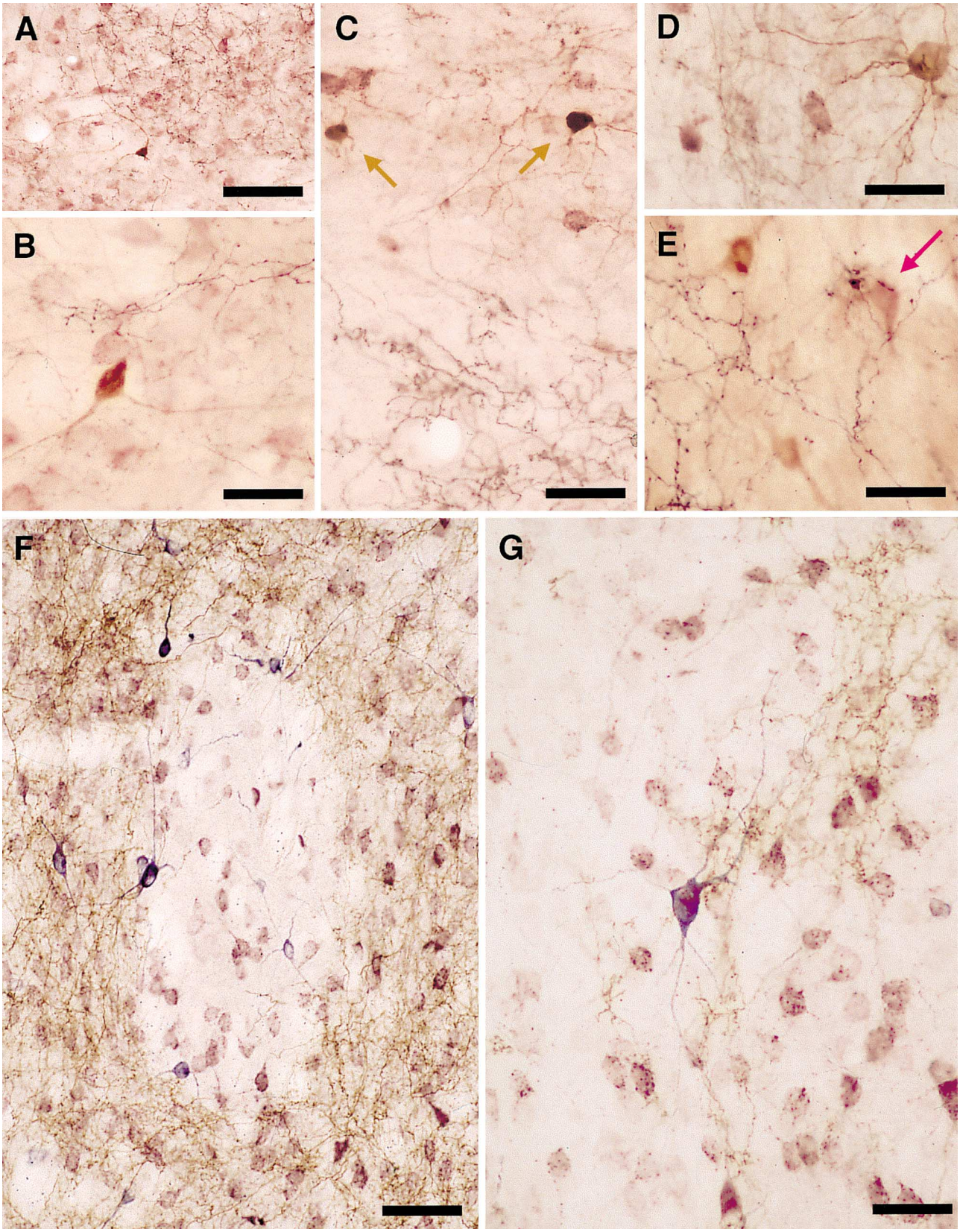

Fig. 2.

tracing with BDA, immunocytochemistry for CR or PV and retrograde tracing with FG also resulted in acceptable staining quality (Fig. 2A–D). Despite some background stain inherent to CR and PV immunocytochemistry, the staining for BDA (DAB-Ni, black), CR or PV (DAB, brown) and FG (V-VIP, purple) provided sufficient resolution between the labeled elements. Only the series aimed at the simultaneous detection of BDA labeled fibers, ChAT-ir interneurons and transported FG failed to produce an acceptable level of resolution (Fig. 2E).

4. Discussion

The present report describes the use of a sequential protocol to visualize projections in one and the same histological preparation with the fine microscopical details of small areas within the striatum. It allows the study of the anatomical relationship of the afferent fibers and the neurons projecting out of the striatum together with chemically identified interneurons. The protocol can be applied to study a variety of delicate neuronal circuits in the striatum and the fiber projections in which these interneurons are presumably involved. These procedures may also be used to shed new light on the architecture of brain circuits in any other brain areas that display a similar relationship between the neuronal elements involved. In order to facilitate the reproduction of this method by others, we will further discuss several technical limitations, pitfalls and drawbacks that in our experience may be encountered.

4.1. Single staining versus triple staining

When attempting triple staining protocols, one should keep in mind that several details will probably be lost when compared with the quality that can be expected from single staining procedures, although the final results might approach the ideal. In our experience, no significant decrease in the staining quality was ever noticed in combining BDA and FG tracing when compared with single tracing procedures. The main differences were observed when additionally the detection of interneurons was attempted. Striatal interneurons probably rank among the most difficult of neurons to be unequivocally identified by means of immunohistochemical methods. Prolonged incubations in the peroxidase substrate were frequently used in order to better appreciate the fine details of a given interneuron, a risky choice that often resulted in the appearance of a moderate amount of background staining. When attempting multiple staining sequences, a priority is to keep the background signal as low as possible. In summary, the investigator is always facing a balance between a minimal level of background stain and the full visualization of the neuronal morphological details. For example, the incubation for the 'diaphorase' staining was concluded before an intense neuropil stain began to appear. A similar criterion was applied to the PV immunocytochemistry.

4.2. Problems that may be encountered

Multiple staining procedures are usually limited by three main drawbacks that are often related to each other: (i) cross-reactions between the antisera involved, (ii) unsupportable levels of background staining and (iii) the phenomenon of 'color mixing' (for a review, see Lanciego et al., 2000). Nowadays, we currently have at our disposal an extensive variety of commercial antisera (primary antisera, bridge antisera and PAP complexes), and as a result, one must choose the antisera to be used carefully to avoid the risks of cross-reactivity between them. As stated previously, the reduction of background staining levels is one of the most critical goals in multiple staining protocols. In our experience, the most efficient tool in keeping the background staining below acceptable levels is the intermittent microscopical examination of the progress of each individual immunoreaction. Finally, the phenomenon of 'color mixing' is undoubtedly the main limitation of any multiple staining method. Color mixing occurs when one of the peroxidase substrates develops the color destined for a second substrate, to be used later in the procedure. The phenomenon is common when cross-reactivity is observed between the antisera involved and also often occurs with prolonged incubations in each peroxidase substrate. In our experience, the best way to minimize the color mixing phenomena is to select carefully the antisera to be used and to closely examine each immunoreaction as it is developing. The appropriate order in which the chromogens are to be used throughout the procedure is being particularly critical. As described here, the best results were obtained by first using the strongest chromogen (DAB-Ni), then the DAB substrate, and finally the weakest chromogen (V-VIP).

Another notorious drawback one may encounter relates to the appearance of the NADPH-d stained neurons as a function of the way in which the fixation process was conducted. The visualization of NADPH-d activity is often hampered when dealing with weakly perfused brains (González-Hernández et al., 1996).

4.3. Limitations of the present study

The present report describes a straightforward method using three peroxidase substrates rendering three different colored precipitates, and was designed to be visualized by light microscopy. When trying to elucidate the relationships between afferent fibers, efferent

neurons and related interneurons, one should undertake ultrastructural studies that exceed the scope of the present report. Anderson et al. (1994) has reported a valuable triple-labeling strategy that permits the use of electron microscopy for this kind of microcircuit. This method comprises the use of DAB, benzidine dihydrochloride and silver-intensified immunogold as the three distinct peroxidase substrates. Another practical choice can be achieved by combining Gold-substituted, silver-enhanced DAB and non-intensified DAB (as reported by Görcs et al., 1986), with the subsequent use of the V-VIP substrate, since the recently introduced V-VIP substrate is characterized by its own electron-dense granular texture (Zhou and Grofova, 1995; Köbbert et al., 2000).

Acknowledgements

Supported by Michael J. Fox Foundation, Fondo de Investigaciones Sanitarias 01/0237, Ministerio de Educación Ref: PM98-0035, Departamento de Salud del Gobierno de Navarra (Ref: 'Beca Ortiz de Landázuri'), Fundación Marcelino Botín and Universidad de Navarra.

References

Albin RL, Young AB, Penney JB. The functional anatomy of basal ganglia disorders. Trends Neurosci 1989;12:366–75.

Anderson KD, Karle EJ, Reiner A. A pre-embedding triple-label electron microscopic immunohistochemical method as applied to the study of multiple inputs to defined tegmental neurons. J Histochem Cytochem 1994;42:49–56.

Bennett BD, Bolam JP. Characterization of calretinin-immunoreactive structures in the striatum of the rat. Brain Res 1993;609:137–48.

Bennett BD, Bolam JP. Synaptic input and output of parvalbumin immunoreactive neurons in the neostriatum of the rat. Neuroscience 1994;62:707–19.

Bolam JP, Clarke DJ, Smith AD, Somogyi P. A type of aspiny neuron in the rat neostriatum accumulates [3H]-aminobutyric acid: combination of Golgi-staining, autoradiography, and electron microscopy. J Comp Neurol 1983;213:121–34.

Bolam JP, Wainer BH, Smith AD. Characterization of cholinergic neurons in the rat neostriatum. A combination of choline acetyltransferase immunocytochemistry, Golgi-impregnation and electron microscopy. Neuroscience 1984;12:711–8.

Chang HT, Wilson CJ, Kitai ST. A Golgi study of rat neostriatal neurons: light microscopic analysis. J Comp Neurol 1982;208:107–26.

Cowan RL, Wilson CJ, Emson PC, Heizmann CW. Parvalbumin-containing GABAergic interneurons in the rat neostriatum. J Comp Neurol 1990;302:197–205.

Deschênes M, Bourassa J, Doan VP, Parent A. A single-cell study of the axonal projections arising from the posterior intralaminar nuclei in the rat. Eur J Neurosci 1996;8:329–43.

Dimova R, Vuillet J, Nieoullon A, Kerkerian-Le Goff L. Ultrastructural features of the choline acetyltransferase-containing neurons and relationships with nigral dopaminergic and cortical afferent pathways in the rat striatum. Neuroscience 1993;53:1059–71.

Figueredo-Cárdenas G, Medina L, Reiner A. Calretinin is largely localized to a unique population of striatal interneurons in rats. Brain Res 1996a;709:145–50.

Figueredo-Cárdenas G, Morello M, Sancesario G, Bernardi G, Reiner A. Colocalization of somatostatin, neuropeptide Y, neuronal nitric oxide synthase and NADPH-diaphorase in striatal interneurons in rats. Brain Res 1996b;735:317–24.

González-Hernández T, Pérez de la Cruz M, Mantolán-Sarmiento B. Histochemical and immunohistochemical detection of neurons that produce nitric oxide: effect of different fixative parameters and immunoreactivity against non-neuronal NOS antisera. J Histochem Cytochem 1996;44:1399–413.

Görcs TJ, Léránth C, MacLusky NJ. The use of gold-substituted silver-intensified diaminobenzidine (DAB) and non-intensified DAB for simultaneous electron microscopic immunoperoxidase labeling of tyrosine hydroxylase and glutamic acid decarboxylase immunoreactivity in the rat medial preoptic area. J Histochem Cytochem 1986;34:1439–47.

Hancock MB. DAB-nickel substrate for the differential immunoperoxidase staining of nerve fibers and fiber terminals. J Histochem Cytochem 1982;32:311–4.

Herkenham M, Pert CB. Mosaic distribution of opiate receptors, parafascicular projections and acetylcholinesterase in rat striatum. Nature 1981;291:415–8.

Hope BT, Vincent SR. Histochemical characterization of neuronal NADPH-diaphorase. J Histochem Cytochem 1989;37:653–61.

Kachidian P, Vuillet J, Nieoullon A, Lafaille G, Kerkerian-Le Goff L. Striatal neuropeptide Y neurones are not a target for thalamic afferent fibres. NeuroReport 1996;7:1665–9.

Kachidian P, Vuillet J, Bartoll M, Castets F, Nieoullon A, Kerkerian-Le Goff L. Relationships between striatin-containing neurons and cortical or thalamic afferent fibres in the rat striatum. An ultrastructural study by dual labelling. Neuroscience 1998;85:111–22.

Kawaguchi Y, Wilson CJ, Augood SJ, Emson PC. Striatal interneurones: chemical, physiological and morphological characterization. Trends Neurosci 1995;18:527–35.

Kita H, Kitai ST. Glutamate decarboxylase immunoreactive neurons in rat neostriatum: their morphological types and populations. Brain Res 1988;447:346–52.

Kita H, Kosaka T, Heizmann CW. Parvalbumin-immunoreactive neurons in the rat neostriatum: a light and electron microscopic study. Brain Res 1990;536:1–15.

Köbbert C, Apps R, Bechmann I, Lanciego JL, Mey J, Thanos S. Current concepts in neuroanatomical tracing. Progr Neurobiol 2000;62:327–51.

Koós T, Tepper JM. Inhibitory control of neostriatal projection neurons by GABAergic interneurons. Nature Neurosci 1999;2:467–72.

Kowall NW, Ferrante RJ, Beal MF, Richardson EP Jr, Sofroniew MV, Cuello AC, Martin JB. Neuropeptide Y, somatostatin, and reduced nicotinamide adenine dinucleotide phosphate diaphorase in the human striatum: a combined immunocytochemical and enzyme histochemical study. Neuroscience 1987;28:817–28.

Kubota Y, Kawaguchi Y. Spatial distribution of chemically identified intrinsic neurons in relation to patch and matrix compartments of rat neostriatum. J Comp Neurol 1993;332:499–513.

Kubota Y, Inagaki S, Kito S, Wu JY. Dopaminergic axons directly make synapses with GABAergic neurons in the rat neostriatum. Brain Res 1987;406:147–56.

Lanciego JL, Goede PH, Witter MP, Wouterlood FG. Use of peroxidase substrate Vector® VIP for multiple staining in light microscopy. J Neurosci Meth 1997;74:1–7.

Lanciego JL, Luquin MR, Guillén J, Giménez-Amaya JM. Multiple neuroanatomical tracing in primates. Brain Res Prot 1998;2:323–32.

Lanciego JL, Wouterlood FG, Erro E, Arribas J, Gonzalo N, Urra X, Cervantes S, Giménez-Amaya JM. Complex brain circuits studied via simultaneous and permanent detection of three transported neuroanatomical tracers in the same histological section. J Neurosci Meth 2000;103:127–35.

Lapper SR, Bolam JP. Input from the frontal cortex and the parafascicular nucleus to cholinergic interneurons in the dorsal striatum of the rat. Neuroscience 1992;51:533–45.

Lapper SR, Smith Y, Sadikot AF, Parent A, Bolam JP. Cortical input to parvalbumin-immunoreactive neurones in the putamen of the squirrel monkey. Brain Res 1992;580:215–24.

Lehmann J, Langer SZ. The striatal cholinergic interneuron: synaptic target of dopaminergic terminals? Neuroscience 1983;10:1105–20.

Mura A, Feldon J, Mintz M. The expression of the calcium binding protein calretinin in the rat striatum: effects of dopamine depletion and L-DOPA treatment. Exp Neurol 2000;164:322–32.

Paxinos G, Watson C. Atlas of the rat brain in stereotaxic coordinates. 4th ed. New York: Academic Press, 1998.

Rosene DL, Roy NJ, Davis BJ. A cryoprotection method that facilitates cutting frozen sections of whole monkey brain for histological and histochemical processing without freezing artifact. J Histochem Cytochem 1986;34:1301–16.

Rudkin TM, Sadikot AF. Thalamic input to parvalbumin-immunoreactive GABAergic interneurons: organization in normal striatum and effect of neonatal decortication. Neuroscience 1999;88:1165–75.

Rushlow W, Flumerfelt BA, Naus CCG. Colocalization of somatostatin, neuropeptide Y and NADPH-diaphorase in the caudate-putamen of the rat. J Comp Neurol 1995;351:499–508.

Sadikot AF, Parent A, François C. The centre median and parafascicular thalamic nuclei project respectively to the sensorimotor and associative-limbic striatal territories in the squirrel monkey. Brain Res 1990;510:161–5.

Sadikot AF, Parent A, François C. Efferent connections of the centromedian and parafascicular thalamic nuclei in the squirrel monkey: a PHA-L study of subcortical projections. J Comp Neurol 1992a;315:137–59.

Sadikot AF, Parent A, Smith Y, Bolam JP. Efferent connections of the centromedian and parafascicular thalamic nuclei in the squirrel monkey: a light and electron microscopic study of the thalamostriatal projection in relation to striatal heterogeneity. J Comp Neurol 1992b;320:228–42.

Sandell JH, Graybiel AM, Chesselet MF. A new enzyme marker for striatal compartmentalization: NADPH diaphorase activity in the caudate nucleus and putamen of the cat. J Comp Neurol 1986;243:326–34.

Satoh K, Staines WA, Atmadia S, Fibiger HC. Ultrastructural observations of the cholinergic neuron in the rat striatum as identified by acetylcholinesterase pharmacohistochemistry. Neuroscience 1983;10:1121–36.

Scherer-Singler U, Vincent SR, Kimura H, McGeer EG. Demonstration of a unique population of neurons with NADPH-diaphorase histochemistry. J Neurosci Meth 1983;9:229–34.

Sidibé M, Smith Y. Differential synaptic innervation of striatofugal neurones projecting to the internal or external segments of the globus pallidus by thalamic afferents in the squirrel monkey. J Comp Neurol 1996;365:445–65.

Sidibé M, Smith Y. Thalamic inputs to striatal interneurons in monkeys: synaptic organization and co-localization of calcium binding proteins. Neuroscience 1999;89:1189–208.

Smith Y, Bevan MD, Shink E, Bolam JP. Microcircuitry of the direct and indirect pathways of the basal ganglia. Neuroscience 1998;86:353–87.

Veenman CL, Reiner A, Honig MG. Biotinylated dextran amine as an anterograde tracer for single- and double-label studies. J Neurosci Meth 1992;55:65–78.

Vincent SR, Johansson O. Striatal neurons containing both somatostatin- and avian pancreatic polypeptide (APP)-like immunoreactivities and NADPH-diaphorase activity: a light and electron microscopic study. J Comp Neurol 1983;217:264–70.

Vincent SR, Staines WA, Fibiger HC. Histochemical demonstration of separate populations of somatostatin and cholinergic neurons in the rat striatum. Neurosci Lett 1983a;35:111–4.

Vincent SR, Johansson O, Hökfelt T, Skirboll L, Elde RP, Terenius L, Kimmel J, Goldstein M. NADPH-diaphorase: a selective histochemical marker for striatal neurons containing both somatostatin- and avian pancreatic polypeptide (APP)-like immunoreactivities. J Comp Neurol 1983b;217:252–63.

Vuillet J, Kerkerian-Le Goff L, Kachidian P, Dusticier G, Bosler O, Nieoullon A. Striatal NPY-containing neurons receive GABAergic afferents and may also contain GABA: an electron microscopic study in the rat. Eur J Neurosci 1990;2:672–81.

Wilson CJ, Groves PM. Fine structure and synaptic connections of the common spiny neuron of the rat neostriatum: a study employing intracellular injection of horseradish peroxidase. J Comp Neurol 1980;194:599–615.

Wu Y, Parent A. Striatal interneurons expressing calretinin, parvalbumin or NADPH-diaphorase: a comparative study in the rat, monkey and human. Brain Res 2000;863:182–91.

Zhou M, Grofova I. The use of peroxidase substrate Vector® VIP in electron microscopic single and double antigen localization. J Neurosci Meth 1995;62:149–58.